

Sensorless DTC of induction motor using improved neural network switching state selector controller

IQBAL MESSAÏF, EL-MADJID BERKOUK and NADIA SAADIA

The paper deals with development of sensorless Direct Torque Control (DTC) system based on neural network. This network is built to solve the task of proper switching states selection based on information about electromagnetic torque and stator flux (position and magnitude) of induction motor. In fact, this technique which uses conventional switching table is not convenient for one-line and real time control for its high computation time. In order to avoid this problem a solution based on neural network is proposed. Well trained Artificial Neural Network structure can replace successfully the switching table. However, in the Neutral-Point-Clamped topology, it has an inherent problem of Neutral Point Potential (NPP) variation. In this way, a Neural Network-Direct Torque Control technique has been applied and the estimated value of the Neutral Point Potential is used, which is calculated by motor currents. This control strategy offers the possibility of selecting appropriate switching state to achieve the control of Neutral Point Potential. Simulation results verify the validity of the proposed method.

Key words: direct torque control, NPC three-level inverter, switching table, neural point potential, neural network, induction motor

1. Introduction

In recent years many studies have been developed to find out different solutions for the induction motor control having the features of precise and quick torque response, and reduction of the complexity of field oriented algorithms. The Direct Torque Control (DTC) technique has been recognized as viable solution to achieve these requirements. The main advantages of DTC are: absence of coordinate transformation and current regulator and absence of separate voltage modulation block. In addition, DTC minimizes the use of motor parameters, so it is very little sensible to the parameters variation [1],[2].

I. Messaïf is with Laboratoire d'Instrumentation, Département d'Instrumentation et Automatique, Faculté d'Électronique et d'Informatique, Université des Sciences et de la Technologie Houari Boumediene, BP no 32 El-Alia 16111 Bab-Ezzouar, Alger, Algérie. E-mail: imessaif@hotmail.com. E-M. Berkouk is with Laboratoire de Commande des Processus, École Nationale Polytechnique d'Alger, 10, rue Hassen Badi, El Harrach, Alger, Algérie. E-mail: emberkouk@yahoo.fr. N. Saadia is with Laboratoire de Robotique Parallélisme et Électroénergétique, Département d'Instrumentation et Automatique, Faculté d'Électronique et d'Informatique, Université des Sciences et de la Technologie Houari Boumediene, BP no 32 El-Alia 16111 Bab-Ezzouar, Alger, Algérie. E-mail: saadia_nadia@hotmail.com.

Received 20.09.2010. Revised 6.12.2010.

The operation with unbalanced voltage in the DC bus affects the Neutral Point Clamped (NPC) converter performance due to the generation of uncharacteristic harmonics in the inverter output voltage. In order to maintain the equal voltage division, it is critical to control the Neutral Point Potential (NPP). A large amount of research has looked at solving of this problem [3],[4],[5].

NPP has the closed relations with the vectors that can be implemented by different switch combinations. Therefore, analysis of the variation of NPP is required and a control method for maintaining the NPP should be developed.

In principle, DTC method bases on instantaneous space vector theory. By optimal selection of the space voltage vectors in each sampling period, DTC achieves effective control of the electromagnetic torque and the stator flux on the basis of the errors between their references and estimated values. It also regulates the NPP through the information on the voltage capacitors. It is possible to directly control the inverter states through a switching table in order to reduce the torque and flux errors within the desired bands limits and also the NPP variations.

Common disadvantage of conventional DTC is the large dimensions of its switching table, particularly in the multilevel inverter [6],[7],[8]. This technique is not convenient for one-line and real-time control. The use of Artificial Neural Networks (ANN) can solve this problem. It has been motivated by their properties of learning capability, speed computation and generalization to improve the control performance of the system and by several advantages over the conventional controllers, such as stability, speed and robustness [9],[10].

The paper is organized as follows: sections 2 and 3 present respectively the three-level inverter NPC topology and the DTC strategy, the analysis of the NPP is developed in next section, the authors study the stability problem of the input DC voltage sources inverter using the redundancy criteria of the available voltage vectors. The structure of ANN and the training method are described at section 5. After perfectly training, this structure achieved the effective input and output control of the DTC system fed by a three-level NPC voltage source inverter (VSI). Finally, conclusion and perspectives are given in the last section.

2. Basic DTC Principles

A block diagram of a basic direct torque control (DTC) controller is given in Fig.1. In principle, DTC is a direct hysteresis stator flux and electromagnetic torque control scheme, which triggers one of the available discrete voltage vectors generated by a VSI to keep the stator flux and torque within the limits of two predefined bands. The correct application of this principle allows a decoupled control of flux and torque [11].

In Direct Torque Control schemes, the magnitude of the stator flux linkage vector is controlled which further can be decomposed to its orthogonal components expressed at a stationary reference frame as:

$$\varphi_{ds} = \int (v_{ds} - R_s i_{ds}) dt \tag{1}$$

$$\varphi_{qs} = \int (v_{qs} - R_s i_{qs}) dt \tag{2}$$

where φ_{ds} and φ_{qs} are d-axis and q-axis stator flux linkage components.

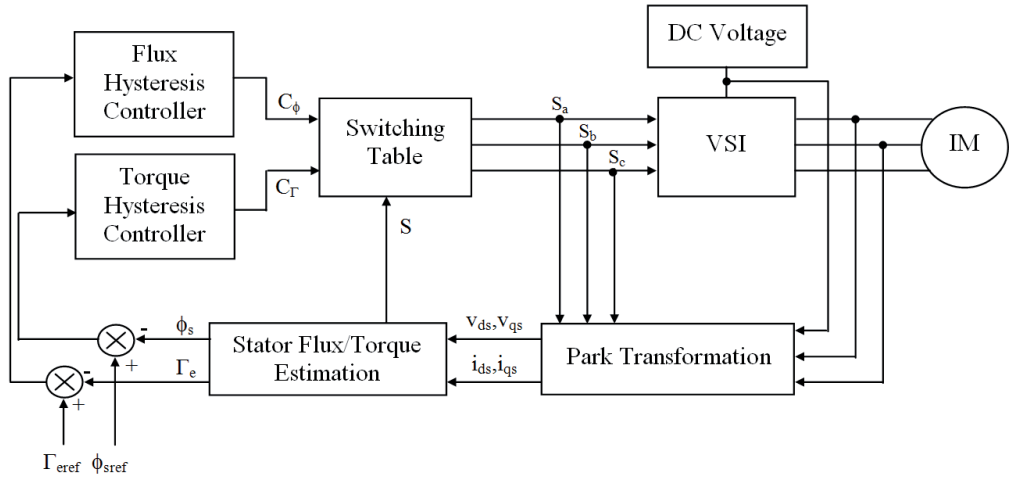


Figure 1. Basic DTC controller.

The torque could be expressed in terms of stator flux, rotor flux and the angle γ between them, i.e.:

$$\Gamma_e = p \frac{L_m}{\sigma L_s L_r} \varphi_s \varphi_r \sin(\gamma) \tag{3}$$

In formula (3) $\sigma = 1 - \frac{L_m^2}{L_s L_r}$, L_m is the magnetizing inductance of the motor, and L_s and L_r are the stator and rotor inductance, respectively.

In general, rotor flux changes much more slower than that of the stator. If sampling period T_e is short enough, and the stator flux is assumed to be constant, the torque can be rapidly changed by tuning γ in the desired direction (Fig. 2). The angle γ can be easily changed by the appropriate space voltage vector.

If for simplicity, it is assumed that the stator voltage drop $R_s i_s$ is small and is neglected, than the stator flux variation can be expressed as:

$$\Delta\varphi_s \approx v_s T_e \tag{4}$$

As shown in formula (4), the stator flux variation is nearly proportional to voltage vector, because the sampling period is constant, and stator flux space vector will move fast if non-zero switching vectors are applied.

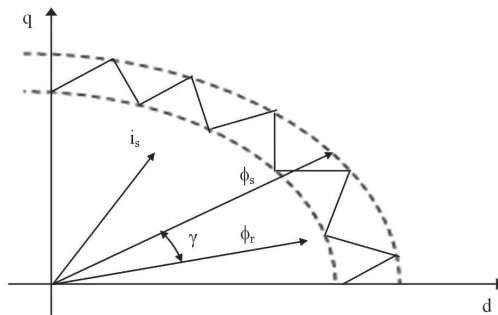


Figure 2. Stator and rotor fluxes and stator current vectors.

If p denotes the number of pole pairs, the original torque equation (equation (3)) has another presentation as follows:

$$\Gamma_e = p(i_{qs}\phi_{ds} - i_{ds}\phi_{qs}). \quad (5)$$

3. Three-level inverter topology and the NPC voltage source

The advantage of the three-level NPC voltage source inverter can be summarized as follows:

- voltage across the switches is only half of the DC bus voltage,
- switching losses are cut in the half with reduced harmonics of output waveforms for the same switching frequency,
- power rating increases.

However, the drawbacks of this kind of inverter is complex control, more devices to be involved, and the charge balance problem of the NPP.

The schematic diagram of this inverter is shown in Fig. 3. It is built-up with twelve switches, each one containing freewheeling diode and six power diodes that allow for connection of the phases outputs to the middle point o . As in the two-level VSI, the necessary conditions for the switching states of the three-level VSI are that the DC link capacitors should not be shorted and each bridge leg has three status: 1, 0 and -1. Switching control S_i can be defined as:

$$S_i = -1 \Rightarrow (S_{i1}, S_{i2}, S_{i3}, S_{i4}) = (0, 0, 1, 1)$$

$$S_i = 0 \Rightarrow (S_{i1}, S_{i2}, S_{i3}, S_{i4}) = (0, 1, 1, 0)$$

$$S_i = 1 \Rightarrow (S_{i1}, S_{i2}, S_{i3}, S_{i4}) = (1, 1, 0, 0)$$

where $i = a, b, c$.

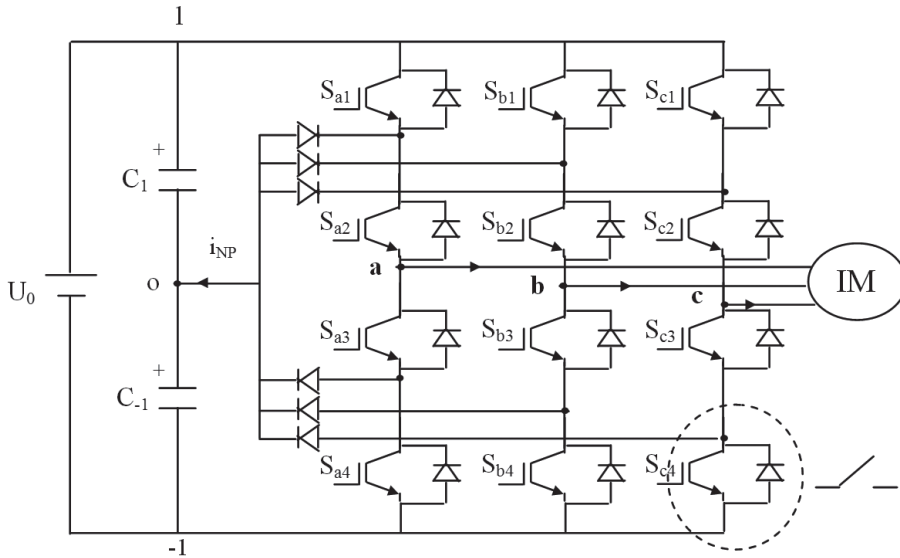


Figure 3. Schematic diagram of a three-level NPC VSI.

Therefore, the stator voltage vector in the Park stationary plane (d,q) might be written as follow:

$$v_s = \sqrt{\frac{2}{3}} \left[v_{aN} + v_{bN}e^{j\frac{2\pi}{3}} + v_{cN}e^{j\frac{4\pi}{3}} \right] \quad (6)$$

where v_{aN} , v_{bN} and v_{cN} represent the stator simple voltages.

Relatively to the two-level inverter which is only capable to produce 8 voltage vectors [10], a three-level inverter has $3^3 = 27$ switching states as Fig. 4 shows. If voltages of two capacitors are equivalent, some switching vectors are overlapped and there are 19 effective vectors. According to the magnitude of the voltage vectors, we divide them into four groups:

The large vectors are the vectors that all of three switches are connected to either off, 1 or -1 potentials except the case of all three are connected at the same point. The medium vectors are the ones that have only one phase connected at neutral point and other two switches are connected to 1 and -1 potential each other. The small vectors have two switches connected at the same point and the remaining one connected at another adjacent point. The zero vectors have all three switches connected to same point. The zero vectors do not have output voltage. Besides, some space vectors as the small ones refer to two different switches configurations (for example 100 and 0-1-1).

Keeping in mind the simplicity of DTC, the same principle, as explained in section 2, can be applied if three-level inverter feeds the induction motor.

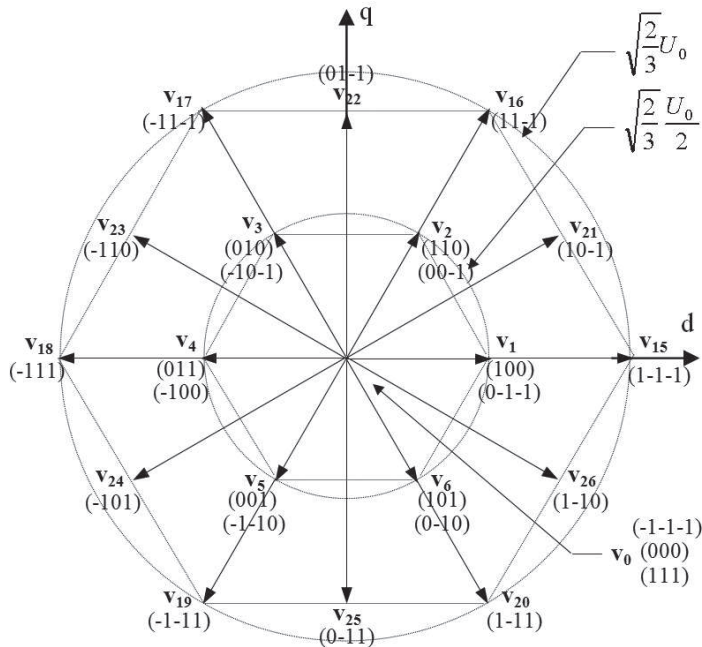


Figure 4. Space voltage vector with their switching states.

For the regulation of the field, let the variable ϵ_ϕ be located in one of the two regions to which variable C_ϕ in two states is associated. The flux control is made by two-level hysteresis controller and C_ϕ defines the action which is wished according to the behavior of the field. Also, for the regulation of the electromagnetic torque, a high level performance torque control is required. To improve the torque control, let of the mismatch ϵ_{Gamma} belongs to one of the five regions, with which a variable C_Γ in five states is associated. The torque control is then controlled by a hysteresis controller built with two lower bounds and two upper known bounds, and C_Γ defines the action which is wished according to the behavior of the torque.

Several switching tables for three-level inverter are presented in literature [6], [7]. An optimal table for the inverter selector has been developed [12], to achieve accurate control. The flux position in the (d,q) plane is quantified in six sectors S of 60° degrees starting with the first sector situated between -30° and 30° . Numbers in the table for inverter state are written according to Fig. 4. In order to simplify the problem, the mechanical rotor speed is considered when assigning the voltage vectors needed at each sectors. The speed of the stator flux linkage vector is given by the modulus of the applied voltage vector. Thus, the voltage vectors are chosen according to the rotor speed [8]. Voltage vectors with low amplitude are chosen for lower speeds. Taking into account available voltage vector amplitudes in a three-level inverter, two different tables have been used. Each table corresponds to a specific speed range, as shown in Table 1.

Table 6. Switching table

		$\Omega < \frac{\Omega_{nom}}{2}$						$\Omega \geq \frac{\Omega_{nom}}{2}$					
		S						S					
C_ϕ	C_Γ	1	2	3	4	5	6	1	2	3	4	5	6
+1	+2	21	22	23	24	25	26	16	17	18	19	20	15
	+1	2	3	4	5	6	1	21	22	23	24	25	26
	0	Zero vector						Zero vector					
	-1	6	1	2	3	4	5	26	21	22	23	24	25
	-2	26	21	22	23	24	25	20	15	16	17	18	19
0	+2	22	23	24	25	26	21	22	23	24	25	26	21
	+1	3	4	5	6	1	2	17	18	19	20	15	16
	0	Zero vector						Zero vector					
	-1	5	6	1	2	3	4	19	20	15	16	17	18
	-2	25	26	21	22	23	24	25	26	21	22	23	24
-1	+2	23	24	25	26	21	22	23	24	25	26	21	22
	+1	3	4	5	6	1	2	17	18	19	20	15	16
	0	Zero vector						Zero vector					
	-1	5	6	1	2	3	4	19	20	15	16	17	18
	-2	24	25	26	21	22	23	24	25	26	21	22	23

(-2/-1/0/+1/+2: high decreases/decreases/equal/increases/high increases)

Note, that the zero vectors are always selected to minimize the commutation number of switches.

4. Analysis of the neutral point potential

The multi-level structure has an inherent problem of NPP unbalance. As the level increases, the problem becomes more complicated. This study concentrates on modeling the properties of DTCs with respect to the current in the neutral point. The direct reason of NPP unbalance is the current flow from/to the neutral point. As mentioned above, NPC three-level inverter has redundant states. Thus, some discrete voltage level can be obtained by more than one switching state. The voltage evolution for a given capacitors are different for each state, as shown in this section. This redundancy permits to control of the capacitors voltages while the requested vector voltage is supplied [13].

The large vectors and the zero vectors do not change the voltage of neutral point. For the medium vector, there is only one vector for a specific direction. The line current flows through the neutral point for a given vector and the NPP is then affected. The compensation of voltage capacitor balance has to be given to the next medium vector because this vector could flow opposite current from the capacitor bank.

Fig. 5 shows example of one small vector given by two different switching combinations. Both combinations produce the same output voltage v_1 , but when the first combination is applied, the current flows into the neutral point and produces discharge in the capacitor C_1 and then follows out and produces a charge in the same capacitor. This property provides the possibility to control the voltage of the neutral point.

Basing on this property, a control strategy will be presented and applied to three level NPC VSI. In Tab. 2, some switching states and the corresponding capacitors voltage evolution are presented. The capacitor voltage evolutions are different at each one of those switching states. Thus, using the required voltage vector as inputs together with the actual state of the capacitor voltages and the current direction in the neutral point, a control algorithm is defined. Then, the inverter will be controlled by the switching state assuming the requested discrete voltage vector and the needed capacitor voltage evolutions. The diagram of the control algorithm is shown in Fig. 6.

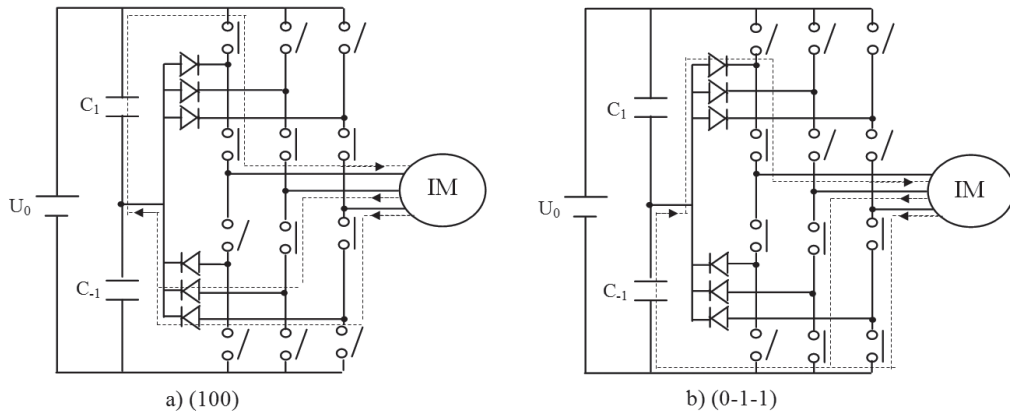


Figure 5. Two different switching combinations of vector v_1 .

In order to realize safe operation of this topology for the three-level inverter, an appropriate method needs to be found for keeping NPP as half of the input voltage.

$$\begin{bmatrix} v_{ab} \\ v_{bc} \\ v_{ca} \end{bmatrix} = \begin{bmatrix} S_{ab1}S_{ab-1} \\ S_{bc1}S_{bc-1} \\ S_{ca1}S_{ca-1} \end{bmatrix} \begin{bmatrix} U_{C1} \\ U_{C-1} \end{bmatrix} \quad (7)$$

Table 7. Effect of small vectors on neutral current and voltage capacitor variation

Positive switching states				Negative switching states			
	i_{NP}	ΔU_{C1}	ΔU_{C-1}		i_{NP}	ΔU_{C1}	ΔU_{C-1}
(1,0,0)	i_a	-	+	(0,-1,-1)	$-i_a$	+	-
(0,0,-1)	i_c	-	+	(1,1,0)	$-i_c$	+	-
(0,1,0)	i_b	-	+	(-1,0,-1)	$-i_b$	+	-
(-1,0,0)	i_a	-	+	(0,1,1)	$-i_a$	+	-
(0,0,1)	i_c	-	+	(-1,-1,0)	$-i_c$	+	-
(0,-1,0)	i_b	-	+	(1,0,1)	$-i_b$	+	-

”+” positive evolution

”-” negative evolution

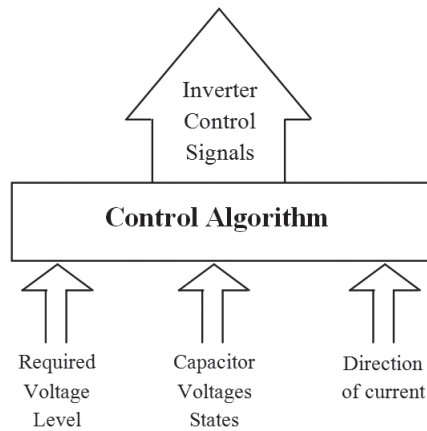


Figure 6. Control algorithm block diagram.

where $S_{ab1} = S_{a1} - S_{b1}$, $S_{ab-1} = S_{a-1} - S_{b-1} \dots$, S_{a1} , S_{b1} , S_{c1} , S_{a-1} , S_{b-1} and S_{c-1} represent the inverter switching functions for the positive (e.g. S_{a1} , S_{a2}) and negative (e.g. S_{a3} , S_{a4}) switches.

The voltage of C_1 and C_{-1} in terms of the full DC link voltage and the neutral point error voltage ϵ_{NP} are written as:

$$\begin{cases} U_{C1} = \frac{U_0}{2} + \epsilon_{NP} \\ U_{C-1} = \frac{U_0}{2} - \epsilon_{NP} \end{cases} \quad (8)$$

The equation that relates the currents i_1 and i_{-1} with the inverter output currents i_a , i_b and i_c is written as follow:

$$\begin{bmatrix} i_1 \\ i_{-1} \end{bmatrix} = \frac{1}{3} \begin{bmatrix} S_{ab1}S_{bc1}S_{ca1} \\ S_{ab-1}S_{bc-1}S_{ca-1} \end{bmatrix} \begin{bmatrix} i_a - i_b \\ i_b - i_c \\ i_c - i_a \end{bmatrix}. \quad (9)$$

One should notice, that $C_1 = C_{-1} = C$ and the neutral current, i_{NP} , is equal to $i_1 + i_{-1}$. We can derive equation (10), which defines the dynamic relationship between i_{NP} and ε_{NP} .

$$i_{NP} = -2C \frac{d\varepsilon_{NP}}{dt}. \quad (10)$$

Finally, combining these equations, a dynamic equation describing the three-level switching network is developed:

$$\frac{d\varepsilon_{NP}}{dt} = -\frac{1}{6C} [S_{ab1} + S_{ab-1}S_{bc1} + S_{bc-1}S_{ca1} + S_{ca-1}] \times \begin{bmatrix} i_a - i_b \\ i_b - i_c \\ i_c - i_a \end{bmatrix} \quad (11)$$

The DTC technique is achieved by alternately selecting one of the available voltage vectors to keep stator flux and electromagnetic flux near the corresponding references and also stabilize the NPP variations. The selection table generates pulses (S_a, S_b, S_c) to control the power switches in the inverter. This technique is not convenient for one-line and real-time control for its high computation time.

5. Networks as a universal approximator

5.1. Switching state selector using ANN

Neural networks can be described as a universal approximation [14]. They approximate complex functions using several layers of neurons, structured in a similar way as the human brain. Artificial Neural Networks (ANN's) possess the virtue of learning and generating. The learning capability makes ANN's very powerful in control applications where the dynamics of a plant or process control is partially known or the mathematical representation is very complicated. The generalization property is very useful because it allows to train neural network with a limited training data set.

Thus, the ANN is trained to simulate complicated relation between the inverter switching states and the errors of the stator flux, output torque and the voltage capacitor. After well trained, it is used as the switching states selector for the DTC of induction motor fed by the three-level NPC VSI.

In our case, the ANN structure needs a minimum of four layers as shown in Fig.7 [12]. The configuration of the input and output layer depend to the problem solving. In

our case, it require five linear input nodes (the outputs of the three controllers flux, torque and voltage capacitor, the stator flux locus plus one information about motor speed, $[C_\Gamma, C_\phi, S, C_U, C_{|\Omega|}]^T$) and three linear output nodes (as $[nn_a, nn_b, nn_c]^T$). $[S_a, S_b, S_c]^T$ represents the desired outputs. Note that the thresholds connected can be considered as weights to be adapted with the training algorithm.

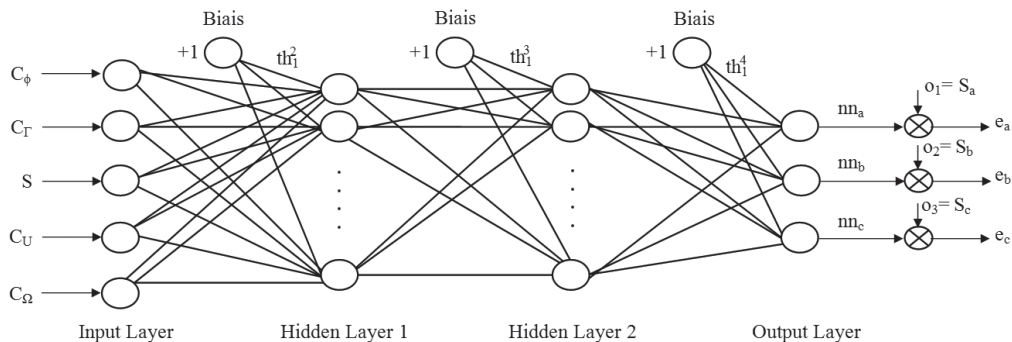


Figure 7. Neural network structure.

5.2. Training algorithm of ANN

The training diagram is presented in Fig. 8. Training data are produced from the conventional switching table (Tab. 1). So, the outputs of the switching table method are compared with the outputs of the ANN, and the error is used to tune the weights of the neural network. The initial weights were chosen randomly within the rang -1 to +1.

The training process is made off-line using the Levenberg-Marquardt (LM) method [15],[16]. This method represent one of the most powerful algorithms for the training of feed-forward networks. It gives a good compromise between the speed of the Newton algorithm and the stability of the steepest descent method.

If the weights of the network are considered as the components of a vector w , the training process involves the determination of this vector which optimizes a performance function E , equation (12). This function can base on the output error or on state criteria for process output. In our case, for K output units ($K = 3$ in our case) and a set of P training patterns, the criteria which is used is given by:

$$E(w) = \sum_{p=1}^P \sum_{i=a,b,c}^K \left(o_i^{(p)} - nn_i^{(p)} \right)^2. \tag{12}$$

Named also Mean Square Error (MSE) cost function, where $nn_i^{(p)}$ and $o_i^{(p)}$ denote respectively the output activations and desired responses, and w is the column vector containing all the weights and the thresholds of the network.

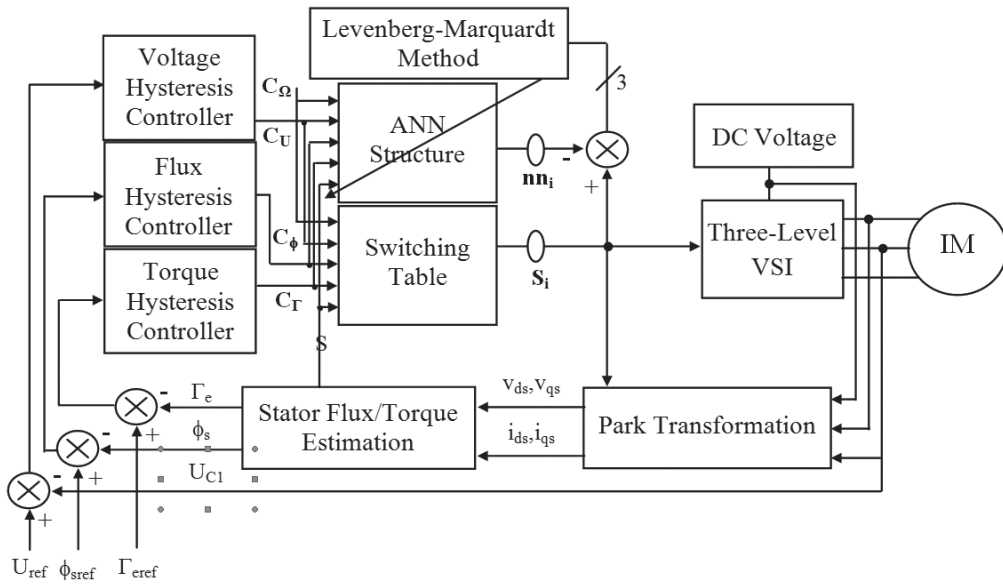


Figure 8. Off-line training block diagram of ANN.

The main idea in second order methods is the local approximation of the cost function by a quadratic form as follows:

$$E(w + \Delta w) = E(w) + \nabla E(w)^T \Delta w + \frac{1}{2} \Delta w^T \nabla^2 E(w) \Delta w \tag{13}$$

where $\nabla E(w)$ and $\nabla^2 E(w)$ are the gradient vector and the matrix of second derivatives (Hessian matrix) of the cost function respectively. The optimal step Δw is obtained by the optimality condition [18]:

$$\Delta w = -[\nabla^2 E(w)]^{-1} \nabla E(w). \tag{14}$$

Due to the special form (sum of squares) of equation (12), the Hessian matrix can be approximate as follows:

$$\nabla^2 E(w) = J^T(w)J(w) + \mu I \tag{15}$$

where $J(w)$ is the Jacobian matrix of first derivatives of the residuals $e_i^{(p)} = (o_i^{(p)} - m_i^{(p)})$, I the identity matrix and μ the learning parameter. For $\mu = 0$, the algorithm becomes Gauss-Newton method. For very large μ the Levenberg-Marquardt algorithm becomes steepest descent or error back-propagation algorithm. This parameter is automatically adjusted at each iteration in order to secure convergence.

The steps involved in training a neural network using LM algorithm are as follows [17]:

1. Present all inputs to the network and compute the corresponding network outputs and errors. Compute the MSE over all inputs as in equation (12).
2. Compute the Jacobian matrix, $J(w)$ where w represents the weights and the thresholds of the network.
3. Solve the Levenberg-Marquardt weight update equation (14) to obtain Δw .
4. Recompute the error using $w + \Delta w$. If this new error is smaller than that computed in step 1, then reduce the training parameter μ by μ^- , let $w = w + \Delta w$, and go back the step 1. If the error is not reduced, then increase μ by μ^+ and go back to the step 3. Parameters μ^- and μ^+ are defined by user.
5. The algorithm is assumed to converged if the norm of the gradient is less than some predetermined value, or when the error has been reduced to some error goal.

6. Simulation results

The optimal configuration in term of precision and computation time leads to a feed-forward neural network type with four layers: 5 input-layer neurons, 12 neurons in the first hidden layer, 12 neurons in the second hidden layer and 3 output-layer neurons [12]. The sigmoid function is used as non-linear activation function for hidden and output layers whereas the linear function is chosen for the input layer.

The training automated with Matlab simulation program and the Levenberg-Marquardt method is developed for this purpose and this structure is trained off-line using all training data obtained from the conventional switching table (Tab. 1). At the end of training process (when an acceptable mean squared error and absolute error between desired and NN outputs are reached, as Figs. 9 and 10 show), the model obtained consists of the weight and threshold vectors, which are summarized in the Appendix.

The three-level DTC strategy without control of the NPP has been tested by simulation, the motor characteristics are shown in the Appendix. All simulations have been obtained with a sample time for the control loop of $100\mu\text{s}$. The voltage of the DC bus is 514V and a constant load torque equal to the nominal value has been applied. The PI controller speed gains are $k_p = 0.83$ and $k_i = 5.82$ respectively.

Fig.11 presents respectively the simulation results of the stator line voltage, capacitors voltage (U_{C1} and U_{C-1}) and the neutral current variations (i_{NP}). The DC link has a capacity of 3.9mF and theirs voltages are unbalanced. The NPP is rising significantly, it may causes overvoltage across the semi-conductor switches and affect the motor performances. Therefore, analysis for the variation of NPP is required and a control method for maintaining this potential point should be developed.

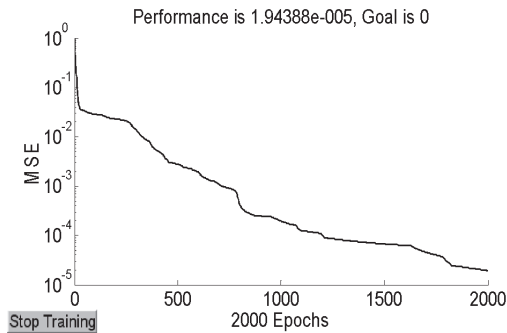


Figure 9. Mean square error for LM training algorithm.

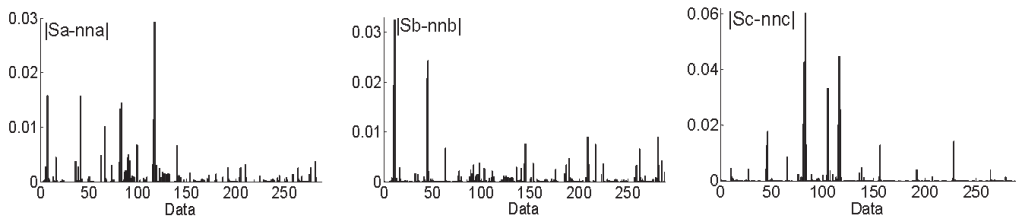


Figure 10. Absolute errors between table and NN outputs.

Also, the results given by the ANN structure are almost the same with these given by the conventional switching table, which shows that the ANN has been properly trained. Therefore, this structure can replace the switching table method to be the output vector selector for the DTC of the three-level inverter-fed induction motor.

Simulation results in a speed control loop of NN-DTC strategy in case where the NPP is controlled, is presented in next figures. A constant load torque equal to nominal value has been applied. The amplitudes of hysteresis band are fixed to $\Delta\phi_s = 3\%$, $\Delta\Gamma_{e1} = 2.7\%$ and $\Delta\Gamma_{e2} = 3\%$.

In Fig.12, the voltage capacitors (U_{C1}, U_{C-1}) are shown. The inverter control algorithm keeps the capacitor voltages between the permitted limits, the slight unbalance, with regard to the exact expected values, is due to the allowed tolerance of $\pm 3\%$ around the exact value. In addition, the NP current has a mean value practically null, however the non symmetric variations of this current is due to that the control is assured exclusively by the large and medium vectors in the second half of switching table.

Furthermore, it is possible to reduce the torque ripple amplitude by approximately twice when compared to a two-level NN-DTC strategy [10] for the same sampling period, as shown in Fig. 13. Besides controlling the electromagnetic torque, DTC also controls the stator flux, whose variation is shown in the same figure. The observed ripple in both electromagnetic torque and flux occurs because hysteresis controllers are used.

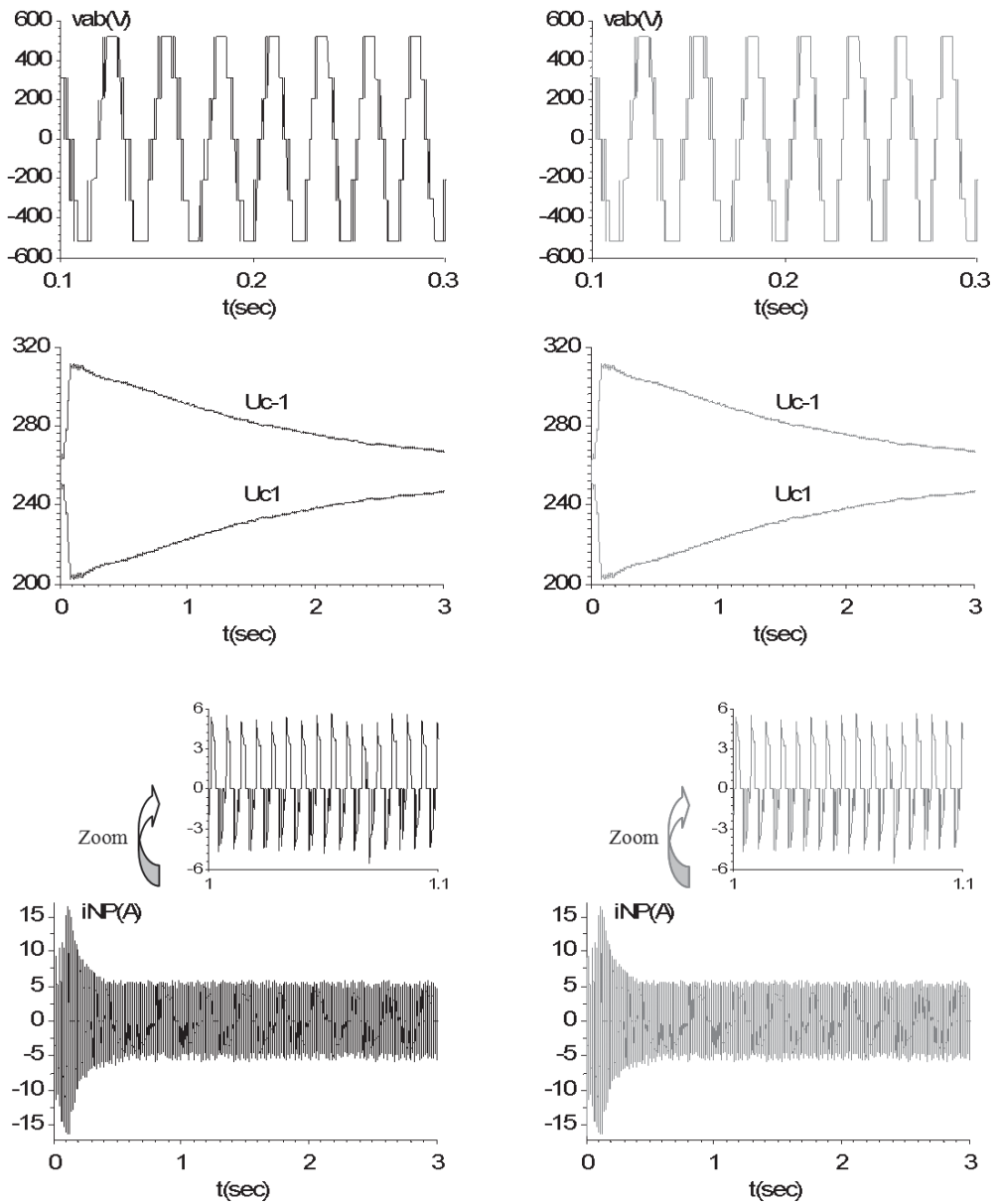


Figure 11. DTC without control of NPP: stator line voltage, deviation of capacitor voltages and neutral point current.

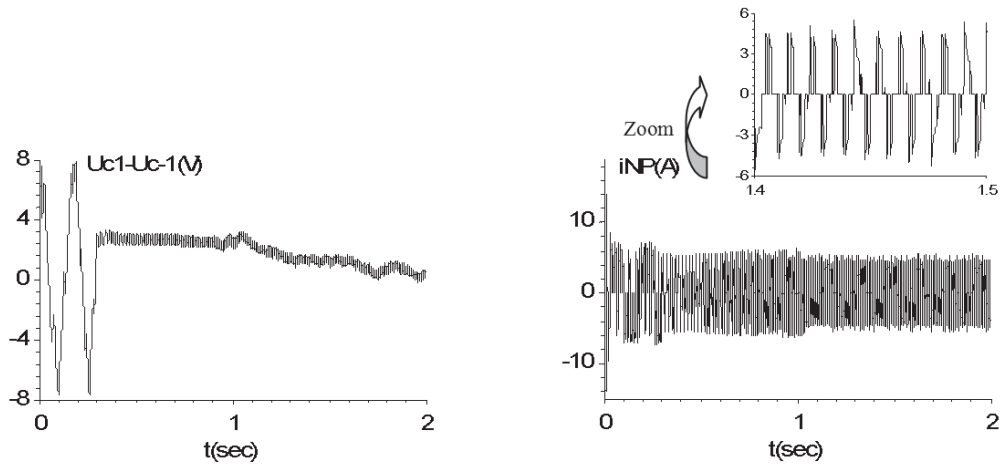


Figure 12. NN-DTC with control of NPP: voltages across the input capacitors, Neutral Point current variations.

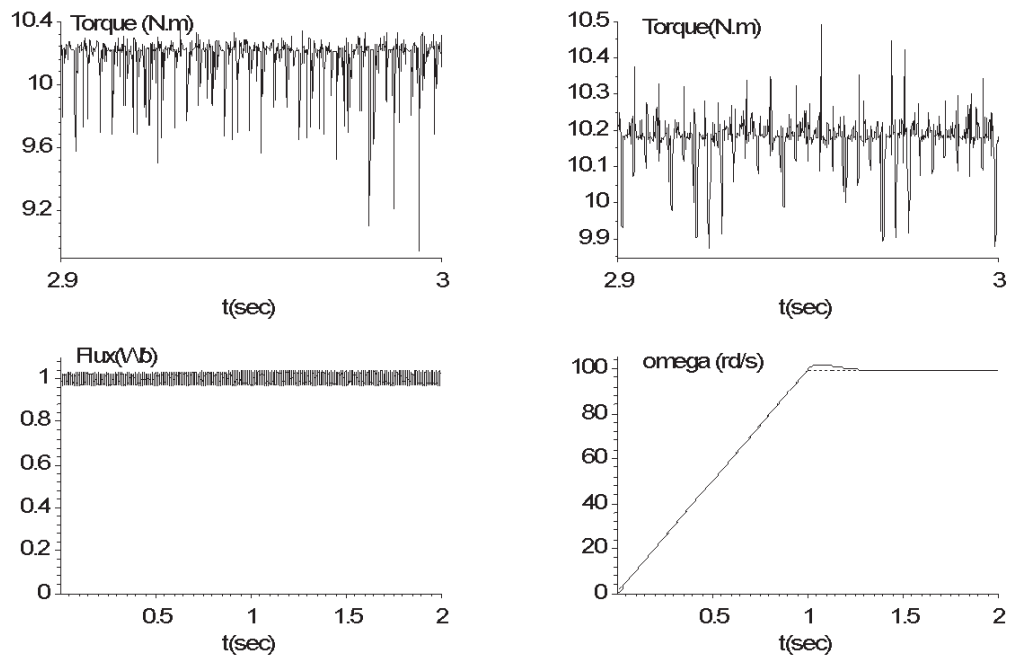


Figure 13. NN-DTC Performances: electromagnetic Torque two-level, three-level NN-DTC strategy, stator flux variation, mechanical speed .

7. Conclusion and perspectives

This research, based on the DTC of induction motor associated with a three-level NPC VSI, proposes using the Artificial Neural Network as the switching table in the DTC system.

The DTC was introduced to give a fast and good dynamic torque of an induction motor. It does not require any mechanical sensor in the rotor comparatively to the conventional methods. Its high dynamic response follows from the absence of the PI current regulator normally used in torque controllers. Also, this control strategy provides easy way to perform the Neutral Point Potential. A precise estimation of the Neutral Point Potential is used to select the appropriate switching state of inverter as shown in switching table. The proposed method provided stabilization of NPP variation and improvement of the motor current waveform. Furthermore, the NPP voltage could be kept with small variation by choosing relatively large capacitors for the capacitor bank.

Because, this technique is not convenient for one-line and real-time control (the implementation of this control strategy requires a great amount of ROM memory, used to store the switching table plus the high computation time), a simplified method to choose the switching states (S_a, S_b, S_c) of the inverter is used. By using the ANN, the selection of the voltage vector becomes much convenient and the switching state can be obtained without any delay when the torque, stator flux and NPP are different from their references. This structure can be trained off-line using all training data obtained from the conventional switching table, this means that once the neural network is trained, it does not need to be trained any more even if the induction motor experiment any change in parameters.

Application of neural network become more important, especially when the level of inverter is increases (3, 5 levels, or more) and theirs switching tables are more complex. In fact, with the increasing number of available voltage vectors of multilevel inverter, it brings difficulty to choose the proper switching state of inverter.

Thus it is important to look at practical implementation system to prove that the proposed structure using ANN is useful, and that it is possible to implement the proposed controller easily. On the other hand, it can be more interesting to associate the fuzzy control in order to determine the inputs of ANN structure. It will be adopted to categorize the flux sector, torque and flux error more rigorous.

References

- [1] V. PETER: Sensorless vector and direct torque control. Oxford university press, London, 1998.
- [2] I. TAKAHASHI and T. NOGUSHI: A new quick-response and high-efficiency control strategy of induction motor. *IEEE Trans. On. IA*, **22**(5), (1986), 820-827.

- [3] F. BOUCHAFAA, A. TALHA, E.-M. BERKOUK and M.S. BOUCHERIT: Stabilization of DC link voltage using a clamping bridge in multilevel cascade. *Int. Conf. on Sciences of Electronic Technologies of Information and Telecommunications*, Tunis, March 27-31, (2005).
- [4] P. PURKAIT and R.S. SRIRAMAKAVACHAM: A new generalized space vector modulation algorithm for neutral-point-clamped multilevel converters. *Symp. on Progress in Electromagnetics Research*, Cambridge, USA, (2006).
- [5] J. HOLTZ and N. OIKONOMOU: Neutral point potential balancing algorithm at low modulation index for three-level inverter medium voltage drives. *IEEE Trans. on Industry Applications*, **43**(3), (2007), 761-768.
- [6] I. MESSAÏF, E.-M. BERKOUK and N. SAADIA: Selection of voltage switching tables DTC of induction motor driven by three-level NPC VSI. *The First Electrical Engineering Conf.*, Aleppo, Syria, 26-28 June, (2007).
- [7] X. DEL TORO, S. CALLS, M.G. JAYNE, P.A. WITTING, A. ARIAS and J.L. POMERAL: Direct torque control of an induction motor using a three-level inverter and fuzzy logic. *Int. Symp. on Industrial Electronics*, **2**, (2004), 923-927.
- [8] I. MESSAÏF, E.-M. BERKOUK and N. SAADIA: DTC strategy of an asynchronous motor fed by a photovoltaic multilevel voltage source inverter. *The Second Int. Conf. on Nuclear and Renewable Energy Resources*, Ankara, Turkey, 4-7 July (2010), 365-371.
- [9] K. HUNT, D. SBARBARO, R. ZBIKOWSKI and P. GOWTHROP: Neural networks for control systems-A survey. *Automatica*, **28**(6), (1992), 1083-1112.
- [10] I. MESSAÏF, E.-M. BERKOUK and N. SAADIA: Direct torque control for induction machines using neural networks. *Archives of Control Sciences*, **17**(1), (2007), 5-16.
- [11] A.L. MOHAMADEIN, R. HAMDY and M. GADOUE: A comparison between two direct torque control strategies for flux and torque ripple reduction for induction motors drives. *Proc. of the Ninth Int. Middle East Power Systems Conf.*, (MEP-CON'2003), Shebeen Al-Koum, Egypt, December 16-18, (2003).
- [12] I. MESSAÏF: Contrôle direct du couple d'une machine asynchrone alimentée par onduleurs multiniveaux par une approche classique et une approche neuronale. Équilibrage des tensions d'entrée des onduleurs. Ph.D thesis. Université des Sciences et de la Technologie Houari Boumediene, Alger, 2009, (in French).
- [13] N. CELANOVIC: Space vector modulation and control of multilevel converters. Ph.D. thesis. Faculty of the Virginia Polytechnic Dept., 2000.
- [14] K. HORNIK: Multilayer networks are universal approximations. *Neural networks*, **2** (1989), 359-366.

- [15] K. LEVENBERG: A method for the solution of certain problems in least squares. *Quarterly of Applied Mathematics*, **5** (1944), 164-168.
- [16] D. MARQUARDT: An algorithm for least squares estimation of nonlinear parameters. *SIAM J. on Applied Mathematics*, **11** (1963), 431-441.
- [17] D. MISHRA, A. YADAV, S. RAY and P.K. KALRA: Levenberg-Marquardt learning algorithm for integrate-and-fire neuron model. *Neural Information Processing-Letters and Reviews*, **9**(2), (2005).

Appendix

Induction machines parameters. The rated values and parameters used in the simulation programs are as follows:

Rated motor power: 1.5kW

Rated speed: 1420 rpm

Rated voltage: 220V

Rated frequency: 50Hz

Stator resistance: 4.85Ω

Rotor resistance: 3.805Ω

Stator inductance: 0.274H

Rotor inductance: 0.274H

Mutual inductance: 0.258H

Pole pairs: 2

Inertia: 0.031kg·m²

Weights and thresholds values

Layer 1

$$th^2 = (-21.997943849780732, -2.8062648671614454, -16.894503302915275, -9.6033891762362185, -15.736466153925884, -21.583693919867514, 3.5863737341303148, -0.76523548382560114, 9.1330602946510862, -7.9168553005742828, -1.81451247757013, 6.8690445297560778)$$

$$w_1^2 = (16.284300265094046, -9.8456073740355414, 1.3116483772530267, 0.040061935169735406, -0.13689840742193785)$$

$$w_2^2 = (-1.42394863344802, 0.69912100584946268, 0.71197398046613958, 1.6475658927935007e-006, 0.80493639585876331)$$

$$w_3^2 = (4.0507582284080579, -6.6671147922321667, 0.58922165007311944, -0.0016861541201888066, 1.9918266439619319)$$

$$\begin{aligned}
 w_4^2 &= (3.9772532145236403, 9.4331444798793935, -1.2380916207911628, \\
 &\quad -0.1084343726615007, 15.589627783184511) \\
 w_5^2 &= (-24.545897368154783, -12.970933424214216, 2.5037897479155249, \\
 &\quad 0.087569752442235693, 3.7320209600938821) \\
 w_6^2 &= (-1.7867881122885343, -12.432916101124835, 0.75758375267679867, \\
 &\quad 0.037311139117969613, 6.2429061696102783) \\
 w_7^2 &= (-0.35691671579914197, -1.673848734979011, 0.17844839137430007, \\
 &\quad -5.7334442617734105, -7.8977065970055369) \\
 w_8^2 &= (0.14595922254006588, -16.662481883099463, 1.2185362275320208, \\
 &\quad 6.2357734820171304e-005, 0.67956948294952424) \\
 w_9^2 &= (-1.3363919925006174, -2.8948335898973756, 0.66818715550394081, \\
 &\quad 6.5207050030231537, -13.896047291025372) \\
 w_{10}^2 &= (-2.311111232887308, -1.8918132667828247, 1.1555992431832216, \\
 &\quad 4.0256069591864751e-005, 0.92565616796595185) \\
 w_{11}^2 &= (0.17675025597846117, -6.0574990149521826, -0.088370774403667432, \\
 &\quad -1.3184481354912387, 8.4103008341388374) \\
 w_{12}^2 &= (1.0386577591057899, -12.474219076014899, -2.1563739165317051, \\
 &\quad 0.14310815958431586, 0.66647628592994546)
 \end{aligned}$$

Layer 2

$$\begin{aligned}
 th^3 &= (-22.676193901849391, -9.003122370538831, -2.6253939470017693, \\
 &\quad 22.334199535130395, 4.5153863470943154, 9.2430763196058656, \\
 &\quad 1.4247357311672042, 3.4673076864141055, 2.1969320165592294, \\
 &\quad -21.055170182724552, 0.14843772786762865, -9.1023820441670527) \\
 w_1^3 &= (-0.46759333239229928, 15.452003209736899, -7.5458437740165767, \\
 &\quad 7.8937851557906944, 0.40247028809580637, -16.610201291162316, \\
 &\quad 0.77503424133802756, 22.565264939852383, 1.1595857973340775, \\
 &\quad 1.8882658351216219, -0.66667189845911845, 0.36886088922902582) \\
 w_2^3 &= (2.505724179120977, -26.451389407666451, 0.11720492719293713, \\
 &\quad -8.9066308168692032, 4.2749596675286492, 9.6339610352944689, \\
 &\quad -0.19043983135791925, -15.373381676315283, 0.37369299491847691, \\
 &\quad -9.3249461505121864, 13.70636394006649, -21.442960845692266) \\
 w_3^3 &= (-2.2281676402207937, 0.10793222582413549, -13.030916857923382, \\
 &\quad 3.0027647234395474, -0.13016964579272552, -0.89058033073265552, \\
 &\quad 2.5133294125682166, 12.107029475697026, 33.815022421690536, \\
 &\quad 13.070546711994716, 35.949817585385041, -8.8495633126207967) \\
 w_4^3 &= (-0.74018870461623065, 12.294701815744725, 14.371699918878504, \\
 &\quad 11.070344294883538, 13.14060110944409, -5.4793483272057513, \\
 &\quad 6.8121694957194769, -2.09213658594365, -12.593589089387052, \\
 &\quad 0.47154107576217574, 1.8009272241385277, 3.8641663856807567) \\
 w_5^3 &= (2.4123038361508327, -9.4431851909242308, 13.071308766140445,
 \end{aligned}$$

$$\begin{aligned}
 & -6.733980777705681, -4.6323837374179231, 14.632955039544461, \\
 & 0.30880854145648945, -4.4495543967548228, 3.901007997740122, \\
 & -10.336160372627797, -0.80176351918139421, -9.9716382194172049) \\
 w_6^3 = & (-21.432225790711129, -11.92379365171433, 2.7356289241925222, \\
 & -0.93968074954168568, -20.276424664886267, 12.26261246595722, \\
 & 1.0364678048853286, 3.7360723637867266, -1.3190554396404646, \\
 & -4.9256114704928082, 7.4372727278576587, -19.086228598504469) \\
 w_7^3 = & (0.29872596798925727, 3.0655473947914138, -0.88493124176032523, \\
 & 0.099124178104921828, 0.9900702303173391, -3.387133141611943, \\
 & -0.65057180299133066, 4.1640536134527757, -1.303060352033504, \\
 & -1.1190313861802155, -2.7362906843564359, 2.5301182362070258) \\
 w_8^3 = & (-11.612411143142829, 17.822840802314317, -11.496470699992056, \\
 & 4.2401650269136928, 0.71758213189710307, 3.3863112562208091, \\
 & 26.844115123412362, 18.695749016720345, 4.3802774061097285, \\
 & -10.020054643907214, 14.981042496008088, 0.2072253908861264) \\
 w_9^3 = & (1.1799916356935791, -0.57342348619627725, 5.9300655974028214, \\
 & 10.133678203548076, 5.8691311310088228, -16.562312072557742, \\
 & -6.4510618189574345, 0.20961008563844402, -5.956194470530729, \\
 & 1.7266287152244764, 3.5034423823176422, -12.708289422796119) \\
 w_{10}^3 = & (-1.408226775504037, -15.378712902460412, -9.0519923081900426, \\
 & 8.6263523035364855, -19.384938201329227, 9.166687204035517, \\
 & 5.843604798537112, -10.356932404964473, 18.661129897145347, \\
 & 11.896078456425553, 13.556033490660276, -7.9738512139018605) \\
 w_{11}^3 = & (4.038128875827323, -7.2919898928641862, 3.3225514051608727, \\
 & -9.9895734785880901, 3.9943295554433504, 8.3732493633661527, \\
 & -8.4292627597658285, -7.5456298172366765, -0.048970310057541745, \\
 & -1.969506732711884, -6.6567510003276498, -1.2213403418421078) \\
 w_{12}^3 = & (8.7689270367951604, -10.463325771618628, -9.5954573712712321, \\
 & 2.8301004984935569, 10.233203165198306, 3.3155683191597629, \\
 & 2.484061781055658, -0.047422502961697845, 2.784040183458437, \\
 & 6.3521176534333899, -6.0183798188665811, 8.1410338717638471)
 \end{aligned}$$

Layer 3

$$\begin{aligned}
 th^4 = & (19.923906817689616, -7.2660320842304076, -25.45406790860882) \\
 w_1^4 = & (14.580467981810571, -23.32798271302952, 21.940897127600131, \\
 & -32.410860544130792, 10.877494699177998, 29.155515582494623, \\
 & -79.21341539804132, -30.726583100041772, -25.696347889949344, \\
 & -32.412209161118639, -48.151109113471115, 10.567488875012431) \\
 w_2^4 = & (12.538529201608728, 42.436556517534051, -36.576659297885321, \\
 & 17.987664625375853, -27.269391733932711, -36.004154302621018, \\
 & 19.896621856678262, 35.988570512484721, -7.9404294813104368, \\
 & 17.987806803556715, 14.205427275156564, -48.736219023745434)
 \end{aligned}$$

$$w_3^4 = (-34.824672367326414, -22.817396700828688, 34.410649907918469, \\ 2.0037322758005147, 6.7215047586859162, 13.49993887771446, \\ 2.2765684337529777, 1.9289750194633457, 21.885350238570204, \\ 2.0038544184099827, -4.133258876178413, 33.951696082529047)$$